Distribution Agreement

In presenting this thesis or dissertation as a partial fulfillment of the requirements for an advanced degree from Emory University, I hereby grant to Emory University and its agents the non-exclusive license to archive, make accessible, and display my thesis or dissertation in whole or in part in all forms of media, now or hereafter known, including display on the world wide web. I understand that I may select some access restrictions as part of the online submission of this thesis or dissertation. I retain all ownership rights to the copyright of the thesis or dissertation. I also retain the right to use in future works (such as articles or books) all or part of this thesis or dissertation.

Signature: Yanyu Wang 03/27/2021

Date

Approval Sheet

Agricultural Greenhouse Gas Emissions under Different Cover Crop Systems

By

Yanyu Wang

Master of Science

Environmental Sciences

Eri Saikawa

Advisor

Carolyn Keough

Committee Member

Debjani Sihi

Committee Member

Accepted:

Lisa A. Tedesco, Ph.D.
Dean of the James T. Laney School of Graduate Studies

Date

Abstract Cover Page

Agricultural Greenhouse Gas Emissions under Different Cover Crop Systems

By

Yanyu Wang

B.S., Colorado State University, 2019

B.S., Anhui Agriculture University, 2019

Advisor: Eri Saikawa, Ph.D.

An abstract of
A thesis submitted to the Faculty of the James T. Laney School of Graduate Studies of Emory University in partial fulfillment of the requirements for the degree of Master of Science in Environmental Sciences
2021

Abstract

Abstract

Agricultural Greenhouse Gas Emissions under Different Cover Crop Systems

By

Yanyu Wang

Cultivated lands that support high productivity have the potential to produce a large amount of GHG emissions, including carbon dioxide (CO_2), nitrous oxide (N_2O), and methane (CH_4). Intensive land management practices can stimulate CO_2, N_2O, and CH_4 emissions from the soil. Cover crop establishment is considered as one of the sustainable land management strategies under warm and humid environmental conditions. To better understand how the incorporation of cover crops affect three major GHGs, in this study, we compared trace gas fluxes in three cover crop systems (CC, CR, and LM) and a no cover crop (Tr) system in a no-till maize field over the whole growing season in 2018. In 2019, we further explored potential differences for the same three GHGs between in-row and between-row of maize for LM and Tr systems during the early growing season. Measurements were taken using a cavity ring-down spectroscopy gas analyzer in Watkinsville, GA. In 2018, the highest fluxes of both CO_2 (6.07 μmol m^{-2} s^{-1}) and N_2O (2.10 μmol m^{-2} hr^{-1}) were from LM between row. The maximum N_2O fluxes observed in LM on June 20th in 2018 was when soil N increase was the largest. Soils served as sinks for CH_4 but Tr system was the smallest CH_4 sink compared to the other three cover crop systems. In our previous work conducted in 2016, we observed a statistically significant difference between LM and Tr only in between the rows of maize. In 2019, however, we observed significantly higher CO_2 emissions in LM compared to Tr, also in the rows of maize. This difference could be related to the difference in measurement techniques and soil C content due to the three-year incorporation of LM. For N_2O, the highest emissions were observed from TrIR (3.93 μmol m^2 hr^{-1}) in 2019 with greater N inputs. In 2019, we observed a smaller CH_4 sink in TrIR (-0.08 μmol m^2 hr^{-1}) compared to TrBWR (-0.61 μmol m^2 hr^{-1}) due potentially to greater NH_4^+ inhibition effects on CH_4 consumption from greater N fertilizer inputs. Comparing four agricultural practices with a net CO_2e in 2018, mitigation effects from CH_4 sink, soil carbon sequestration, reduced fertilizer and herbicide application are still not capable of counteracting higher CO_2 and N_2O emissions generated in the field. The net CO_2e from CC, CR, WC, and Tr were 17,323, 17,129, 30,101, and 11,402 kg ha^{-1} yr^{-1}, respectively.

Cover Page

Agricultural Greenhouse Gas Emissions under Different Cover Crop Systems

By

Yanyu Wang

B.S., Colorado State University, 2019

B.S., Anhui Agriculture University, 2019

Advisor: Eri Saikawa, Ph.D.

A thesis submitted to the Faculty of the James T. Laney School of Graduate Studies of Emory University in partial fulfillment of the requirements for the degree of Master of Science in Environmental Sciences

2021

Acknowledgments

I would firstly express my sincere appreciation to my advisor, Dr. Eri Saikawa, who supported me continuously throughout my two years of master's studies at Emory University. Her expertise and insightful feedback helped me to train my critical thinking ability and brought the thesis work to a higher level. Without her patience and timely feedback, the goal of this study will not be realized. I would also like to thank Dr. Debjani Sihi and Dr. Carolyn Keogh for serving committee members and their valuable guidance in revising the thesis.

I would also like to acknowledge our colleagues: Dr. Nick Hill and Jill Mullican at the University of Georgia for providing us with the soil data. Their participation and inputs help us better understand the results in-depth.

Finally, I must express my special gratitude to my parents for providing me with both financial and emotional supports throughout my years of study. This accomplishment would not have been realized without them.

TABLE OF CONTENTS

List of Figures

List of Tables

Introduction

Human activities, mainly driven by economic and population growth since the industrial revolution, have led to an unprecedented increase in anthropogenic greenhouse gas (GHG) emissions, including carbon dioxide (CO_2), methane (CH_4), and nitrous oxide (N_2O). The atmospheric mixing ratio of CO_2 has increased by 48% since 1750: from 277 parts per million (ppm) in 1750 to 410 ppm in 2019 (Friedlingstein et al., 2020). This rapid increase in CO_2 is largely due to fossil fuel combustion, gas flaring, and cement production (IPCC, 2014). CO_2 emissions from fossil fuel combustion and industrial processes accounted for 78% of total GHG emissions increases from 1970 to 2010. At the same time, CO_2 emissions from forestry and land-use change have also increased by 40% since 1970 (IPCC, 2014).

The mixing ratio of N_2O has similarly increased by more than 20% in the recent decades: from 270 parts per billion (ppb) in 1750 to 331 ppb in 2018 (Tian et al. 2020). N_2O emissions are also the primary factor causing anthropogenic stratospheric ozone depletion (IPCC, 2013, Ravishankara et al, 2009). Anthropogenic emissions account for 30-45% of the total N_2O globally, mainly from agricultural soils and fossil fuel combustion (Fowler, 2009; IPCC, 2013). Agriculture serves as a vital source of N_2O, contributing approximately 50% of total anthropogenic N_2O emissions (IPCC, 2007; Shcherbak et al., 2014). Contribution from agricultural soils primarily results from the addition of synthetic N fertilizer and manure application (Shcherbak et al., 2014).

The mixing ratio of CH_4 has more than doubled from 722 ppb in 1750 to 1857 ppb in 2018 (Saunois et al., 2020). Natural and anthropogenic activities are both responsible for a rapid increase in CH_4 emissions. Natural sources mainly stem from wetlands, and human-induced sources include rice cultivation, landfill, livestock, fossil fuel mining, and hydrocarbon use (IPCC, 2007; Ussiri, 2009). The major consumption pathway of CH_4 is to react with the hydroxyl radical (OH) in the troposphere, while microbial uptake in the soil also acts as a smaller CH_4 sink (IPCC, 2013). Both production and consumption of CH_4 derive from biological processes.

Agricultural production systems are essential for providing food and energy needs, but they are also significant sources of GHG emissions. According to the statistics of global GHG emissions by economic sector, Agriculture, Forestry and Other Land Use (AFOLU) accounted for 24% of total emissions, of which 10-14% came directly from agriculture (Paustian et al., 2016, Smith et al., 2014, Tubiello et al., 2015). Generally, the Global North has higher GHG contributions (35%) in agriculture than the Global South (12%) at the national level (Smith et al., 2014, Wollenberg et al., 2016). Within the United States (U.S.), agriculture accounts for 9% of the total U.S. GHG emissions in 2017 (USEPA, 2017).

Extensive research shows that different land management practices have various effects on three major GHGs: CO_2, CH_4, and N_2O. For CO_2, deforestation, and land-use conversion results in removing stored soil organic carbon (SOC) and releasing CO_2 into the atmosphere (Aydinalp & Cresser, 2008). CO_2 could also be released through soil disturbance events, such

as intensive tillage by accelerating oxidation and decomposition processes (Johnson, 2018). A common practice of burning crop residue after harvest also produces significant CO_2 emissions (Aydinalp & Cresser, 2008).

For N_2O, cultivated lands that support high productivity have the potential to produce a large amount of N_2O emissions based on excessive nitrogen (N) inputs (Paustian et al. 2016). N_2O is produced mainly by microbial activities from nitrification and denitrification processes (Signor & Cerri, 2013). Ammonium-based fertilizer inputs stimulate the nitrification process where ammonium (NH_4^+) is oxidized to nitrate (NO_3^-) under a series of reactions during the nitrification process that also produce N_2O. N_2O can also be generated during the denitrification process as an intermediate product where NO_3^- is used as the terminal electron acceptor. These processes are usually stimulated by N fertilizer applications. Excessive N inputs exceeding plant demands are also susceptible to leaching into adjacent surface and water areas, causing further N_2O emissions (Signor & Cerri, 2013).

For CH_4, microbial activities that participate in the CH_4 production processes are strongly affected by land management practices and environmental conditions, such as mineral N addition, fertilizer rate, tillage intensity, moisture, and temperature, affecting the balance of CH_4 production and consumption (Snyder et al., 2009). CH_4 is generated or used under two antagonistic processes: methanogenesis and methanotrophy. CH_4 is produced under methanogenesis, where organic matter is mineralized through methanogenic archaea under anoxic conditions. Methanotrophy refers to the oxidation of CH_4 to CO_2 with either methanotrophic bacteria or archaea under both anerobic and aerobic conditions. The balance between methanogenesis and methanotrophy determines if the terrestrial environment is a CH_4 source or a sink.

Cover crop, as one of the sustainable agricultural practices, could be established under warm and humid environmental conditions. Cover crops could improve soil quality through increasing SOC and preventing soil erosion. Soils with cover crops can act as carbon sinks by increasing formation of soil organic matter from cover crop residues (Johnson, 2018). Studies suggest that cover crops with N-fixing capability could provide available N to cash crops without additional N inputs (Andrews et al., 2018, Schomberg et al., 2006, Turner et al., 2016). Even cover crops without having the ability to fix N is considered to scavenge the excessive nitrate in the soil and thereby reduce leaching and N_2O emissions from denitrification (Jarecki et al., 2009; Smith and Tiedje, 1979). However, studies found that increases in N_2O after incorporating cover crops sometimes outweigh the mitigation effects from increased SOC, because mineral N fixed by legume cover crop can stimulate N_2O emissions under denitrification (Mitchell et al., 2013; Basche et al., 2014). Increased C inputs from cover crop biomass can also enhance CO_2 emissions. How the incorporation of different types of cover crop influence CO_2 and N_2O emissions is, however, still not well understood. Living mulch (LM) is a recently emerging cover crop system. Different from other cover crop treatments which are killed before the planting of cash crops, LM uses leguminous cover crops maintained throughout the whole growing season (Andrews et al., 2018; Zemenchik et al., 2000). There are also conflicting findings as to whether LM would increase or decrease N_2O emissions (Turner et al. 2016; Gomes et al. 2009; Peters et al. 2020).

In addition to the impacts on CO_2 and N_2O emissions, there is no simple characterization on how the inputs of cover crop residue will impact CH_4 emissions or uptake capacity. Kim et al. (2012) found that higher CH_4 emissions were observed in cover crops with high C/N ratio due to their higher labile C content, which stimulated CH_4 emissions under anaerobic conditions (Le Mer and Roger, 2001; Lu et al., 2000). Conversely, Boeckx and Van Cleemp (1996) observed that residue with low C/N led to high CH_4 emissions due to elevated amount of NH_4^+ and NO_2, which have strong inhibition effects on CH_4 uptake. Meanwhile, previous studies revealed that N fertilizer addition, such as urea, usually exhibits inhibitory effects on CH_4 consumption (Bronson & Mosier, 1994; Conrad & Rothfuss, 1991; Dunfield & Knowles, 1995). So far, it is relatively unknown how N pool in the soil and C/N ratio in cover crop will impact CH_4 uptake.

Based on the complexities of how the incorporation of different cover crops will influence three major GHGs, Peters et al. (2020) conducted some experiments in 2016 and 2017 to explore these effects. From 2016 to 2017, trace gas fluxes (CO_2 and N_2O) were measured in between-row in crimson clover (CC), cereal rye (CR), LM using white clover, and traditional (Tr) under a maize system and in-row CO_2 was also measured among those four treatments. In their study, researchers used a portable infrared gas analyzer (IRGA) (6400XT, Li-Cor) for CO_2 and gas chromatography with mass spectrometry (GC-MS) for CO_2 and N_2O. Peters et al. (2020) found that LM showed both highest CO_2 and N_2O fluxes in both 2016 and 2017 compared to other treatments. Moreover, significantly higher CO_2 emissions were observed in between the rows of maize, where clover was present, than in the rows of maize in the LM system in 2016. However, they were unable to detect CH_4 fluxes.

To better understand how the incorporation of different agricultural practices affect three major GHGs, we continued our study in 2018 and 2019 but with *in-situ* measurements, using a cavity ring-down spectroscopy gas analyzer (Picarro G2508, Santa Clara, CA, USA). Our first primary research question was: how are GHG fluxes differ among CC, CR, LM, and Tr, including CH_4? Secondly, under the same technique (LM or Tr), are three GHGs generated in the rows of maize significantly different from those in between the row? In this study, we measured continuous trace gas fluxes (CO_2, N_2O, and CH_4) and compared them in three cover crop systems (CC, CR, and LM) and a no cover crop (Tr) system in a no-till maize field over the whole growing season in 2018. In 2019, In order to further explore potential differences for all three major GHGs between in-row and between-rows of maize, we focused on in-row and between-row measurements for LM and Tr systems and conducted more intensive daily measurements surrounding the two fertilization periods in the early growing season.

Methods

Site Description and Experimental Design

The study site was located at the West Unit of the University of Georgia's J. Phil Campbell Sr. Resource and Education Center in Watkinsville, GA, USA. More details regarding the location of research station can be found in Peters et al. (2020). This site has been established

for agricultural research since 1937 (Melancon, 2014). Our experiment in 2018 consisted of twelve 6.1×7.3m plots in no-till maize fields, three each for four treatments: 1) with dead crimson clover (CC) cover crop; 2) with dead cereal rye (CR) cover crop; 3) living much (LM) system, with white clover intercrop; and 4) traditional system (Tr), with bare soil (Figure 1). Within each plot, three chambers were placed to account for soil heterogeneity. The surface area and volume of the chamber were 0.0182 m^2 and 2.92 m^3, respectively. Each cycle of sample collection consisted of taking CO_2, N_2O, and CH_4 measurements from nine chambers (three chambers per plot from three plots) in between the rows of maize over 81 minutes. We measured the accumulation of trace gases from nine chambers in one cycle using a multiplexer, taking a sample for 1.5 minutes per chamber, rotating over nine different chambers six times in a cycle. We typically sampled four cycles to measure from all chambers on a sampling day. We quantified soil GHG flux weekly over the whole growing season in 2018. The last day of measurement (September 13) were taken after the maize was harvested. We used this day's observation as a baseline value and removed it from significant tests for GHG fluxes. In 2018, CC, CR, and Tr received two fertilizer applications on April 20 and May 18 at the rate of 50, 250, and 250 kg ha^{-1}, respectively. LM did not receive any N inputs. All four treatments were applied 20mm irrigation equally on Jun 11, Jun 22, July 6, and July 31.

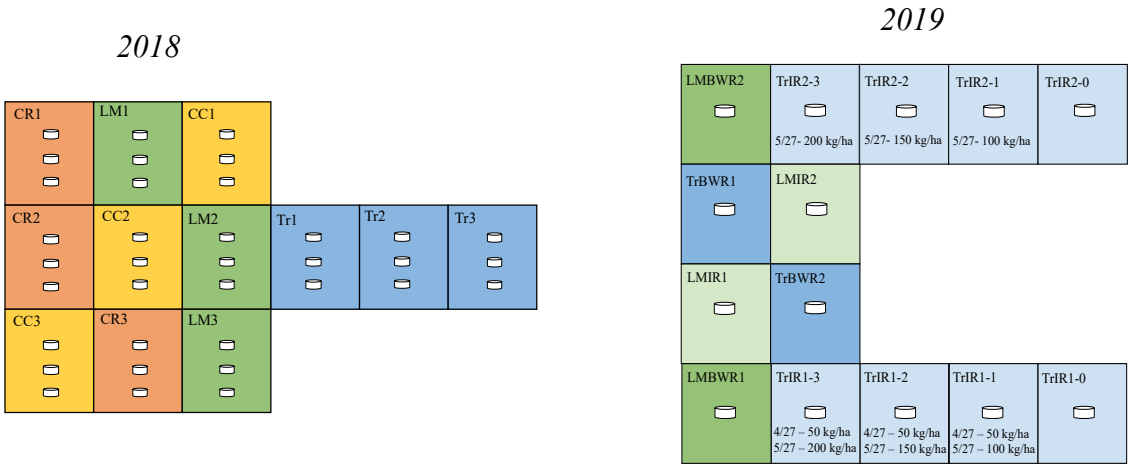

Figure 1. Experimental design in 2018 and 2019. In 2018, our design consisted of three replicate plots of each agriculture practices (CC: yellow, CR: red, LM: green, Tr: blue). In 2019, our design consisted of 14 plots: two plots for Traditional between-row (TrBWR), Living mulch in-row (LMIR), and Living mulch between-row (LMBWR) each (TrBWR: blue; LMIR: light green; LMBWR: green), as well as eight plots for Traditional in-row (TrIR) with varying N fertilizer inputs marked by light blue. Details regarding the N fertilizer amount and dates are labeled.

In 2019, we conducted an intensive field campaign observing daily soil GHG fluxes at an early growing season, with a focus around the two fertilization periods. We measured same gases under Tr and LM systems, with a focus on comparing the in row and between the rows of maize, consisting of the following: a) traditional in row (TrIR); b) traditional between row (TrBWR); c) living mulch in row (LMIR); and d) living mulch between row (LMBWR) (Figure 1). Our experiment in 2019 consisted of fourteen plots in no-till maize fields, two each for TrBWR, LMIR, and LMBWR, and remaining eight plots for TrIR. Within each plot, one chamber was established to measure CO_2, N_2O, and CH_4 fluxes. Each cycle of sample

collection consisted of taking measurements from seven chambers (four chambers from TrIR, and one chamber per plot from three treatments: TrBWR, LMIR, and LMBWR) and seven ambient filters for each chamber over 84 minutes. We measured the accumulation of trace gases from seven chambers in one cycle using a multiplexer, taking a sample for 1 min per chamber, another 1 min measuring the ambient air and rotating that sequence for seven different chambers six times in a cycle. We typically sampled two cycles to measure from all chambers on a sampling day.

LMIR received N fertilizer at the rate of 35 kg ha^{-1} on April 27, while both TrBWR and LMBWR did not receive any. For TrIR, eight plots were established to explore GHG flux variations depending on different fertilization amounts and times. TrIR was separated into TrIR1 and TrIR2 with different fertilization rates. In TrIR1, all four paired plots were fertilized twice during our measurement campaign. On April 27, all four plots (TrIR1-0, TrIR1-1, TrIR1-2, and TrIR1-3) received N fertilizer at the rate of 50 kg ha^{-1}. In addition, four plots in TrIR1 also received fertilizer on May 27 ranging from 0-200 kg ha^{-1} (TrIR1-0: 0 kg ha^{-1}; TrIR1-1: 100 kg ha^{-1}; TrIR1-2: 150 kg ha^{-1}; TrIR1-3: 200 kg ha^{-1}). In TrIR2, all four plots only received fertilizer once on May 27, and the rate ranged from 0-200 kg ha^{-1} (TrIR2-0: 0 kg ha^{-1}; TrIR2-1: 100 kg ha^{-1}; TrIR2-2: 150 kg ha^{-1}; TrIR2-3: 200 kg ha^{-1}). Irrigation events occurred on May 3, when 20mm water was applied to all four treatments.

Soil sampling and GHG flux measurements

We used the G2508 Picarro concentration analyzer to measure the accumulation of trace gases in the chambers. The working principle of Picarro G2508 is based on cavity ring-down spectroscopy (CRDS). CRDS technology utilizes the beam that enters into the ring-down cavity formed by two or more high-reflectivity mirrors (G2508 Gas Concentration Analyzer, n.d.). Three mirrors are used in the Picarro concentration analyzer to sustain the continuous traveling wave. Trace gases such as CO_2, N_2O, and CH_4 have their unique absorption spectrum within the near-infrared range. By measuring the absorption intensity under this wavelength, it can determine the concentration of a specific gas (G2508 Gas Concentration Analyzer, n.d.). CRDS extends the effective pathlength for absorbing up to several kilometers, and the sensitivity of gas concentration can reach parts per billion level in a few seconds (G2508 Gas Concentration Analyzer, n.d.). With the CRDS technique, Picarro has the capability to measure CO_2, N_2O, CH_4, NH_3, and H_2O simultaneously and ensures the data collection under high temporal resolution (G2508 Gas Concentration Analyzer, n.d.). We used water-corrected trace gas mixing ratios for analysis.

Other studies have found a relationship between soil GHG fluxes and other variables, such as soil water content, soil temperature, and total amount of soil C and N (Steenwerth & Belina, 2008; Franzluebbers, 2015; Camarotto et al., 2018). CS625 reflectometers (Campbell Scientific) were used to measure soil moisture and temperature data. CS625 reflectometers were placed in the corn rows at two different soil depths (0-15cm and 0-30cm). The length of the rods is 30cm and the rods were installed at an angle of 30 degrees from the surface. Soil moisture and temperature data were collected at a 10-minute interval to calculate hourly averages. Total soil C and N amounts were measured weekly in May and June and monthly in

July and August. Clover biomass and corresponding soil N content were also measured in all LM plots in 2018 to investigate the effects of clover residue decomposition on N_2O emission spikes at the late growing season. Meteorological data were obtained from a weather station located near experimental plots. Surface pressure and atmospheric temperature were used to calculate soil GHG flux.

Data analysis

Trace gas flux calculation was carried out, using Interactive Data Language (IDL). The mixing ratio [μmol mol^{-1}] of trace gases was first converted, following the Ideal Gas Law (1), where P is surface pressure [atm], R is a gas constant 8.205 x 10^{-5} [$m^3 atm\ mol^{-1}\ K^{-1}$], and T is atmospheric temperature [℃]. Trace gas fluxes [μmol m^2 s^{-1} or μmol m^2 hr^{-1}] were then calculated by the following equation using the change in a gas mixing ratio over a specific time period (1), where t denotes the time period [s or hr], V represents a chamber volume (2.92 [m^3]), and A represents chamber surface area (0.0182 [m^2]) (Collier et al., 2014).

$$Flux = Mixing\ ratio \times \frac{P \times V}{R*(273+T)*A*t} \quad (1)$$

Since CO_2 mixing ratio is greater in magnitude, the flux unit of CO_2 is calculated in [μmol m^{-2} s^{-1}], while changes of N_2O and CH_4 are calculated in [μmol m^{-2} hr^{-1}].

Statistics

All the statistical analyses in this study were performed using R 3.6.1 (R Core Team, 2019). Prior to statistical analysis, normality of all fluxes was assessed using Shapiro-Wilks test (Das & Imon, 2016). Mean CO_2 flux in 2018 was transformed by taking the power of -1/3 and mean CO_2 flux in 2019 was transformed by taking the power of -1/2 to meet the normality, as log transformation failed to meet the normality test for both years. ANOVA and Tukey's pairwise comparison was further implemented for transformed CO_2 flux to investigate which specific agricultural practices were statistically different in their means. Welch t test was carried out for N_2O and CH_4 fluxes due to the failure of meeting normality assumption for all the attempted transformations. Means of N_2O and CH_4 fluxes were compared to explore if there were significant differences between two sets of data. GHG fluxes among the four practices were also compared between different time periods. In 2018, we also analyzed soil GHG emissions from four practices in early and late growing seasons separately. In 2019, we also analyzed GHG fluxes in the first and the second fertilization periods separately. Net CO_2 eq was calculated and compared among four practices (CC, CR, LM, and Tr) in 2018, including CO_2, N_2O and CH_4 fluxes generated in the field, soil labile carbon, as well as carbon equivalent estimates due to the consumption of fertilizer, irrigation and herbicides (Lal. 2004). For three major GHGs, net CO_2e were calculated by firstly converting three major GHGs' units from [μmol m^{-2} s^{-1} or μmol m^{-2} hr^{-1}] to [kg ha^{-1} yr^{-1}]. After that, we used global warming potential (GWP) for a 100-year time horizon to standardize three major GHGs' different climate impacts. N_2O and CH_4 have 298, and 28 times GWP compared to CO_2, respectively (IPCC, 2014). In addition, land management practices for agriculture also lead to GHG emissions into atmosphere. Lal (2004) summarized the estimates of carbon equivalence (CE) for different farm operations: 1.35kg CE for per kg N fertilizer use, 6.3kg CE for per kg herbicides use, and

103kg CE for applying 20mm water irrigation. We calculated net CO_2e for N fertilizer and herbicides use (kg) based on the area of our study plots. Each agricultural practice occupies an area of 133.59 m^2.

Results

GHG fluxes in 2018

We calculated fluxes of three major GHGs (CO_2, N_2O, and CH_4) by conducting measurements weekly in between the rows of maize from the four different agricultural practices during the maize growing season in 2018 (Figure 2). The overall transformed average CO_2 flux showed a significant difference among the four practices (all $p < 0.001$, Table 2). Similar to the findings in Peters et al. (2020), between-row measurements from LM were observed to produce statistically higher CO_2 emissions compared to CC, CR, and Tr, all at $p < 0.001$ level. In this study, the other two cover crop systems (CC and CR) also emitted significantly higher CO_2 emissions than in Tr (Table 1), which was not observed in Peters et al. (2020). Between leguminous (CC) and non-leguminous (CR) cover crops, CO_2 produced were not statistically different (Table 2).

Table 1. Average and standard deviation (n = 368 for each gas species) of trace gas fluxes (CO_2: μmol m^2 s^{-1}, N_2O and CH_4: μmol m^2 hr^{-1}) for four systems in 2018.

Treatment	*CO_2*	*N_2O*	*CH_4*
CC	4.01±3.52	1.23±1.86	-1.07±0.59
CR	4.10±3.39	1.46±4.45	-0.88±0.51
LM	6.07±3.78	2.10±3.65	-0.98±0.65
Tr	2.73±1.61	1.18±1.61	-0.72±0.44

Table 2. Mean transformed CO_2 flux (n = 368) group comparisons from four treatments in 2018.

Groups	*Difference (μmol m^{-2} s^{-1})*	*95% CI Lower bound*	*95% CI Upper bound*	*p value*
		2018		
CR-CC	-0.0032	-0.05	0.04	0.99
LM-CC	-0.081	-0.12	-0.04	1.7×10^{-5} ***
Tr-CC	0.070	0.03	0.11	8.7×10^{-5} ***
LM-CR	-0.078	-0.12	-0.03	4.2×10^{-5} ***
Tr-CR	0.074	0.03	0.12	3.8×10^{-5} ***
Tr-LM	0.15	0.11	0.19	$< 1.0 \times 10^{-7}$ ***

*p < 0.05, **p < 0.01, ***p < 0.001

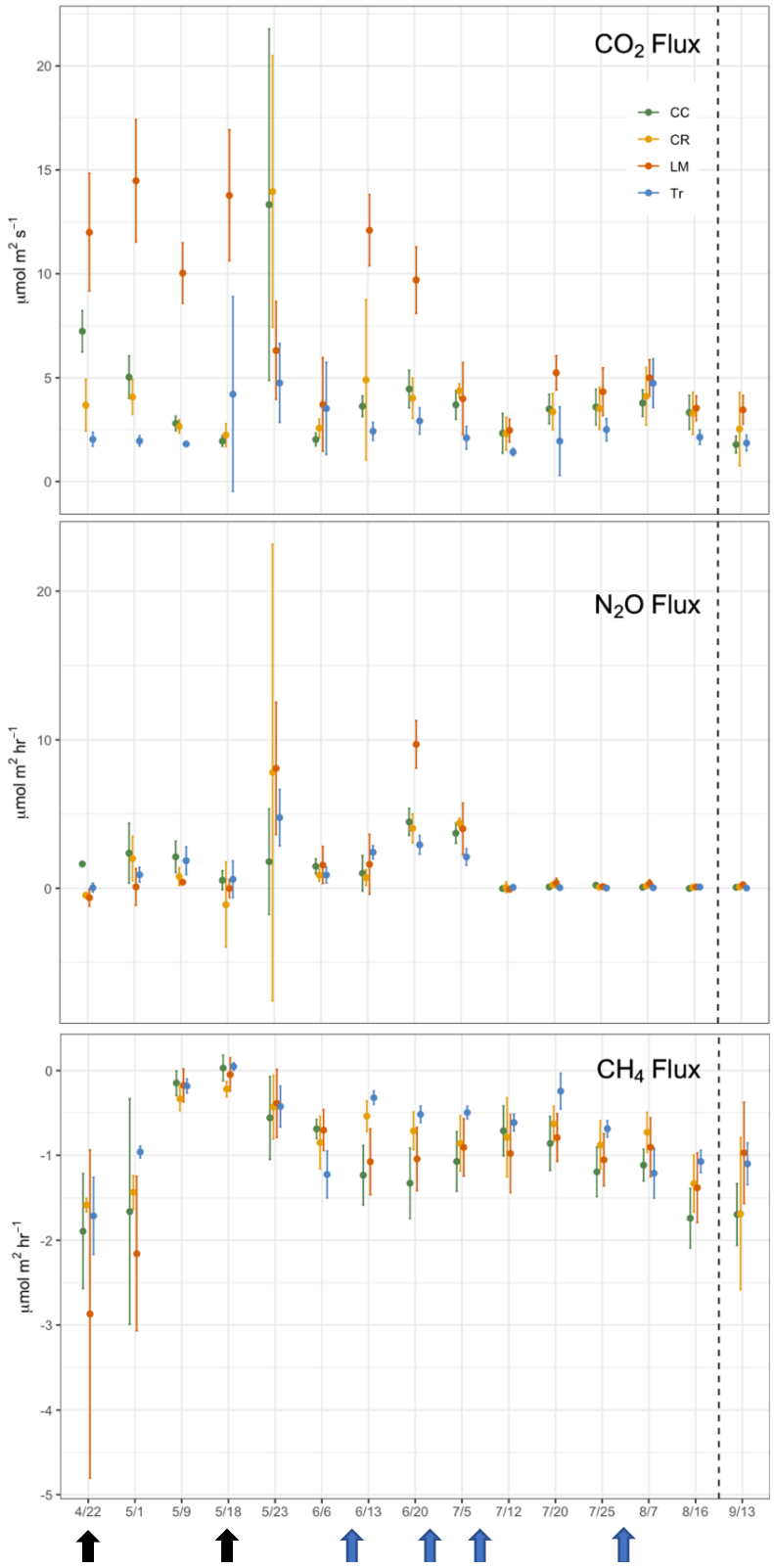

Figure 2. Temporal changes of daily average GHG flux (CO_2, N_2O, and CH_4) measurements between the maize rows in 2018 growing season for crimson clover (CC), cereal rye (CR), white clover living mulch (LM), and conventional (Tr) practices. Black arrows represent twice fertilizer application (4/22 and 5/18) and blue arrows represent four irrigation events (6/11, 6/22, 7/6, and 7/31).

N_2O flux from Tr increased on May 23rd after receiving fertilizer inputs (Figure 2). Greater fluxes were also observed in LM on June 20th (Figure 2), which was most likely due to the elevated soil N added from the decomposing white clover. We measured higher overall N_2O emissions from LM (2.10 μmol m^2 hr^{-1}), with the difference of 0.93 μmol m^2 hr^{-1} compared to Tr (Table 3, $p < 0.05$). In 2018, N_2O emissions from LM were only statistically significantly higher than Tr. This is different from Peters et al. (2020), where LM was found to emit significantly higher N_2O fluxes than CC, CR, and Tr in both 2016 and 2017. In our study, soils in CC and CR plots emitted lower N_2O compared to those in LM but no significant difference was observed (CC-LM: 0.051 μmol m^2 hr^{-1}; CR-LM: 0.3 μmol m^2 hr^{-1}, Table 3). Similar to the past findings, N_2O fluxes in CC and CR were not statistically significantly different from those in Tr (CC-Tr: 0.83 μmol m^2 hr^{-1}; CR-Tr: 0.57 μmol m^2 hr^{-1}, Table 3).

Table 3. Mean N_2O flux Welch t test (n = 368) between certain two treatments among four systems in 2018.

Groups	*Difference (μmol m^{-2} hr^{-1})*	*95% Lower CI*	*95% Upper CI*	*t*	*df*	*p-value*
			2018			
CC-CR	-0.22	-1.26	0.80	-0.44	114.03	0.66
CC-LM	-0.87	-1.75	0.004	-1.97	126.54	5.1×10^{-2}
CC-Tr	0.055	-0.44	0.55	0.22	166.25	0.83
CR-LM	-0.64	-1.87	0.58	-1.04	163.78	0.30
CR-Tr	0.28	-0.72	1.28	0.56	102.26	0.57
LM-Tr	0.93	0.089	1.76	2.19	110.52	3.0×10^{-2} *

*p < 0.05, **p < 0.01, ***p < 0.001

Soils in all four systems exhibited as CH_4 sinks (Figure 2). Tr showed a significantly lower CH_4 uptake rate (-0.72 μmol m^2 hr^{-1}) compared to the other three cover crop systems (Tr-CC: $p < 0.001$; Tr-CR: $p < 0.05$; Tr-LM: $p < 0.01$, Table 4). CC (-1.07 μmol m^2 hr^{-1}) and LM (-0.98 μmol m^2 hr^{-1}) served as larger sinks compared to other treatments and the two did not differ significantly ($p = 0.33$). Comparing CH_4 uptake capacity between leguminous (CC) and non-leguminous cover crop (CR), CC exhibited a significantly larger CH_4 sink compared to CR, with the difference of 0.2 μmol m^2 hr^{-1} ($p < 0.05$, Table 4). LM did not exhibit a significantly larger CH_4 sink compared to CR (LM-CR: p =0.25, Table 4).

Table 4. Mean CH_4 flux Welch t test (n = 368) between certain two treatments among four systems in 2018.

Groups	*Difference (μmol m^{-2} hr^{-1})*	*95% Lower CI*	*95% Upper CI*	*t*	*df*	*p-value*
			2018			
CC-CR	-0.20	-1.07	-0.029	-2.31	165.4	2.2×10^{-2} *
CC-LM	-0.090	-0.28	0.095	-0.97	167.91	0.33
CC-Tr	-0.35	-0.50	-0.20	-4.63	150.3	7.9×10^{-6} ***
CR-LM	0.11	-0.072	0.28	1.17	161.79	0.25
CR-Tr	0.16	0.29	-0.021	-2.27	167.44	2.4×10^{-2} *
LM-Tr	-0.26	-0.42	-0.10	-3.22	142.93	1.6×10^{-3} **

*p < 0.05, **p < 0.01, ***p < 0.001

Both CO_2 and N_2O fluxes were much lower in mid-July and August compared to the earlier parts of the growing season (Figure 3). At the same time, CH_4 sink was also larger in the latter half of the growing season than earlier parts (Figure 3). We thus separated the whole growing season into early (April 22nd – July 5th) and late (July 12th – August 16th) periods to explore GHG flux variations among the four treatments better. During the early period, the average CO_2 flux emitted in CC, CR, LM, and Tr were 5.07 ± 4.83, 5.18 ± 4.55, 8.45 ± 4.25, and 3.01 ± 1.76 μmol m^2 s^{-1}, respectively (Table 5, Figure 3). In the late period, the average CO_2 flux emitted in CC, CR, LM, and Tr were 3.25, 3.26, 3.96, and 2.55 μmol m^2 s^{-1}, respectively (Table 5). As found during the whole growing season, the differences between LM and each of the three other agricultural treatments were statistically significantly different in both periods (LM-CC: $p < 0.01$; LM-CR: $p < 0.001$; LM-Tr: $p < 0.001$, Table 6). Moreover, both CC and CR also emitted higher CO_2 emissions than Tr in both periods as found during the whole growing season (Table 6).

Table 5. Average and standard deviation of trace gas fluxes (CO_2: μmol μmol m^2 s^{-1}, N_2O and CH_4: μmol m^2 hr^{-1}) for four systems in early (n= 179) and late (n= 162) growing seasons in 2018.

	CO_2	N_2O	CH_4
Early growing season (April 22 - July 5)			
CC	5.07 ± 4.83	2.54 ± 2.02	-0.91 ± 0.65
CR	5.18 ± 4.55	2.95 ± 6.14	-0.73 ± 0.43
LM	8.45 ± 4.25	4.25 ± 4.39	-0.91 ± 0.82
Tr	3.01 ± 1.76	2.47 ± 1.63	-0.62 ± 0.47
Late growing season (July 12 – August 16)			
CC	3.25 ± 0.16	0.07 ± 0.16	-1.15 ± 0.47
CR	3.26 ± 1.13	0.11 ± 0.19	-0.90 ± 0.40
LM	3.96 ± 1.28	0.14 ± 0.24	-1.05 ± 0.41
Tr	2.55 ± 1.47	0.10 ±0.14	-0.77 ± 0.39

Table 6. Mean CO_2 flux Welch t test between certain two treatments among four systems in early (n = 179) and late (n= 162) growing seasons in 2018.

Groups	Difference (μmol m^{-2} hr^{-1})	95% Lower CI	95% Upper CI	t	df	p-value
2018 Early growing season (April 22 – July 5)						
CC-CR	-0.071	-2.15	2.00	-0.068	78.452	0.95
CC-LM	-3.38	-5.39	-1.38	-3.36	76.97	1.2×10^{-3} **
CC-Tr	2.06	0.45	3.66	2.58	46.383	1.3×10^{-2} *
CR-LM	-3.31	-5.24	-1.39	-3.43	79.494	9.7×10^{-4} ***
CR-Tr	2.13	0.62	3.63	2.84	48.72	6.5×10^{-3} **
LM-Tr	5.44	4.04	6.84	7.81	50.227	3.2×10^{-10} ***
2018 Late growing season (July 12 – Aug 16)						
CC-CR	0.0024	-0.47	0.47	0.010	73.83	0.99
CC-LM	-0.70	-1.21	-0.20	-2.76	70.07	7.3×10^{-3} **
CC-Tr	0.71	0.18	1.24	2.65	75.93	9.7×10^{-3} **
CR-LM	-0.71	-1.25	-0.16	-2.59	74.82	1.2×10^{-2} *
CR-Tr	0.71	0.14	1.27	2.48	80.78	1.5×10^{-2} *
LM-Tr	1.41	0.81	2.01	4.70	82	1.0×10^{-5} ***

*p < 0.05, **p < 0.01, ***p < 0.001

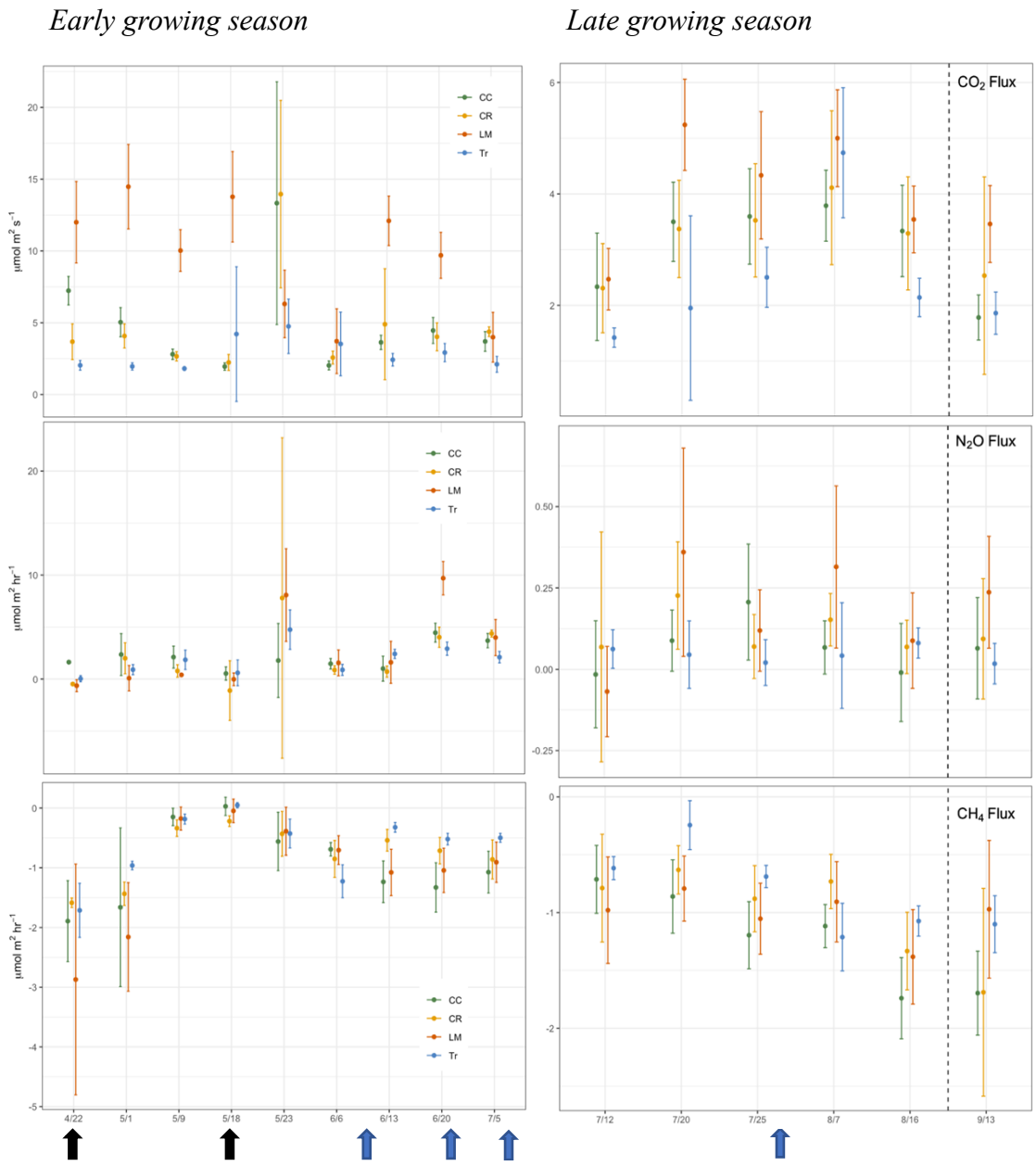

Figure 3. Temporal changes of daily average GHG flux (CO_2, N_2O, and CH_4) measurements during early and late growing season between the maize rows in 2018 growing season for crimson clover (CC), cereal rye (CR), white clover living mulch (LM), and conventional (Tr) treatments. Black arrows represent twice fertilizer application and blue arrows represent irrigation events (4/27 and 5/18) and blue arrows represent four irrigation events (6/11, 6/22, 7/6, and 7/31).

We measured the highest N_2O emissions from the LM system in both early and late growing seasons compared to other three practices (early: 4.25 μmol m^2 hr^{-1}, late: 0.14 μmol m^2 hr^{-1}, Table 5). N_2O emissions generated in LM was significantly higher than those in Tr in both periods separately (early: LM-Tr: 2.00 μmol m^2 hr^{-1}, $p < 0.01$; late: 0.09 μmol m^2 hr^{-1}, $p < 0.05$). In the early period, we measured significantly higher N_2O emissions from LM compared to CC with the difference of 1.71 μmol m^2 hr^{-1}($p < 0.05$, Table 7), although this difference was not observed in the late growing season. Differences in N_2O fluxes between leguminous cover crop (CC) and non-leguminous cover crop (CR) did not differ significantly in either periods (early: $p = 0.69$; late: $p = 0.32$, Table 7). Similar to what was observed for CO_2 flux, larger amount of N_2O was produced in the early growing season in all the four practices.

Table 7. Mean N_2O flux Welch t test between certain two treatments among four systems in early (n = 179) and late (n = 162) growing seasons in 2018.

Groups	Difference (μmol m^{-2} hr^{-1})	95% Lower CI	95% Upper CI	t	df	p-value
2018 Early growing season (April 22 – July 5)						
CC-CR	-0.41	-2.44	1.63	-0.40	48.75	0.69
CC-LM	-1.71	-3.22	-0.19	-2.25	56.50	2.8×10^{-2} *
CC-Tr	0.29	-0.48	1.06	0.76	72.42	0.45
CR-LM	-1.30	-3.65	1.05	-1.10	72.44	0.27
CR-Tr	0.70	-1.28	2.68	0.71	44.10	0.48
LM-Tr	2.00	0.55	3.45	2.78	48.02	7.8×10^{-3} **
2018 Late growing season (July 12 – Aug 16)						
CC-CR	-0.040	-0.12	0.041	-0.99	73.9	0.32
CC-LM	-0.070	-0.16	0.022	-1.51	67.33	0.14
CC-Tr	0.016	-0.04	0.075	0.52	59.19	0.60
CR-LM	-0.029	-0.13	0.069	-0.60	72.98	0.55
CR-Tr	0.056	-0.01	0.12	1.64	53.55	0.11
LM-Tr	0.085	0.004	0.17	2.10	48.46	4.1×10^{-2} *

*p < 0.05, **p < 0.01, ***p < 0.001

Soils in all four treatments functioned as CH_4 sinks. Lower CH_4 uptake rate for Tr was only observed in comparison with the N-fixing cover crop systems – CC and LM – in both early and late growing seasons (Table 8). In addition, the difference was more statistically significant in the late growing season than early for both (Table 8). Similar to the findings for the whole growing season, larger CH_4 sink was not observed in LM compared with CC and CR among the three cover crop systems (Table 8). Between leguminous cover crop (CC) and non-leguminous cover crop (CR), larger CH_4 sink was observed in CC compared with CR only in the late growing season (early: CC-CR: $p = 0.16$; late: CC-CR: $p < 0.05$, Table 8).

Table 8. Mean CH_4 flux Welch t test between certain two treatments among four systems in early (n = 179) and late (n = 162) growing seasons in 2018.

Groups	Difference ($\mu mol\ m^{-2}\ hr^{-1}$)	95% Lower CI	95% Upper CI	t	df	p-value
2018 Early growing season (April 22 – July 5)						
CC-CR	-0.17	-0.42	0.07	-1.41	67.43	0.16
CC-LM	0.01	-0.32	0.34	0.06	75.73	0.95
CC-Tr	-0.29	-0.52	-0.05	-2.38	66.41	2.0×10^{-2} *
CR-LM	0.18	-0.11	0.47	1.26	60.31	0.21
CR-Tr	-0.11	-0.29	0.07	-1.24	90.34	0.22
LM-Tr	-0.29	-0.58	-0.01	-2.07	58.49	4.3×10^{-2} *
2018 Late growing season (July 12 – Aug 16)						
CC-CR	-0.24	-0.44	-0.05	-2.46	74.28	1.6×10^{-2} *
CC-LM	-0.10	-0.30	0.10	-0.97	74.54	0.34
CC-Tr	-0.38	-1.15	-0.77	-4.00	74.02	1.5×10^{-4} ***
CR-LM	0.15	-0.04	0.33	1.60	75.99	0.11
CR-Tr	-0.14	-0.31	0.04	-1.56	79.43	0.12
LM-Tr	-0.28	-0.46	-0.11	-3.23	79.09	1.8×10^{-3} **

*p < 0.05, **p < 0.01, ***p < 0.001

GHG fluxes in 2019

We conducted an intensive daily measurement campaign surrounding the two fertilization periods (April 27 – May 4 and May 23 – June 1) during the early growing season in 2019. We calculated daily GHG fluxes for a week around the two fertilization periods both in between the rows of maize and in the rows of maize from Tr and LM plots (Figure 4). In the first fertilization period (April 27- May 4), LMIR received N fertilizer inputs at the rate of 35 kg ha^{-1}, and three chambers in TrIR1 (TrIR1-1, TrIR1-2, TrIR1-3) also received N fertilizer at the rate of 50 kg ha^{-1}. In the second fertilization period (May 23- June 1), six chambers in TrIR received N fertilizer ranging from 0-200 kg ha^{-1}. LMBWR and TrBWR did not receive any N addition in either periods. Higher CO_2 and N_2O fluxes were observed in the second fertilization period compared to the first fertilization (Figure 5). At the same time, CH_4 sink was also larger in the second fertilization period than the first (Figure 5). We thus first compared GHG fluxes during the whole measurement period for TrIR, TrBWR, LMIR, and LMBWR, then separated the measurements in 2019 into the first fertilization period (April 22nd – July 5th) and second (July 12th – August 16th) to explore how GHG fluxes generated in between the rows of maize and in the rows of maize from Tr and LM plots varied in the two fertilization periods.

We observed the highest CO_2 emissions from LMBWR (7.85 $\mu mol\ m^2\ s^{-1}$, Table 9) in 2019 as found in Peters et al. (2020) in 2016 and 2017. Peters et al. (2020) found that higher CO_2 flux in LM compared to Tr was only observed in between the rows of maize, where clover was present but not within rows in 2016. However, in 2019, higher CO_2 emissions were observed in both LMIR and LMBWR compared to TrIR and TrBWR, respectively (both $p <$ 0.001, Table 10). In both first and second fertilization periods, we measured the highest CO_2 emissions in LMBWR (5.51 $\mu mol\ m^2\ s^{-1}$, 10.70 $\mu mol\ m^2\ s^{-1}$, Table 9). All four practices (TrIR, TrBWR, LMIR, and LMBWR) showed increased CO_2 emissions during the second fertilization period than the first, especially for LMBWR (Figure 5). The CO_2 difference between LMIR and LMBWR increased in the second fertilization period than the first (first: LMBWR-LMIR:

1.31 µmol m^2 s^{-1}; second: LMBWR-LMIR: 6.58 µmol m^2 s^{-1}, Table 11).

Table 9. Average and standard deviation (n = 217 for each gas species) of trace gas fluxes (CO_2: µmol µmol m^2 s^{-1}, N_2O and CH_4: µmol m^2 hr^{-1}) for four measurements in 2019.

Treatment	*CO_2*	*N_2O*	*CH_4*
TrIR	2.23 ± 0.66	3.93 ± 8.53	-0.08 ± 1.01
TrBWR	2.10± 0.96	1.39 ± 1.64	-0.61 ± 0.20
LMIR	4.16 ± 1.15	1.95 ±2.36	-0.35 ± 0.52
LMBWR	7.85 ± 2.91	1.87 ±2.28	-0.52 ± 0.22

Table 10. Mean transformed CO_2 flux group comparisons from four treatments in 2019.

Groups	*Difference (µmol m^{-2} s^{-1})*	*95% CI Lower bound*	*95% CI Upper bound*	*p value*
		2019		
LMIR-LMBWR	0.13	0.06	0.20	4.5×10^{-5} ***
TrBWR-LMBWR	0.37	0.29	0.44	$< 1 \times 10^{-7}$ ***
TrIR-LMBWR	0.31	0.25	0.37	$< 1 \times 10^{-7}$ ***
TrBWR-LMIR	0.24	0.17	0.31	$< 1 \times 10^{-7}$ ***
TrIR-LMIR	0.18	0.13	0.24	$< 1 \times 10^{-7}$ ***
TrIR-TrBWR	-0.06	-0.11	0.0009	0.56

*p < 0.05, **p < 0.01, ***p < 0.001

Table 10. Average and standard deviation of trace gas fluxes for four systems in first (n = 119) and second (n = 98) fertilization periods in 2019.

	CO_2	N_2O	CH_4
	First fertilization period (April 27 - May 4)		
TrIR	1.98 ± 0.65	2.23 ± 3.15	0.25 ± 1.25
TrBWR	1.44 ± 0.78	0.41 ± 0.54	-0.58 ± 0.13
LMIR	4.20 ± 1.48	2.33 ± 3.03	-0.26 ± 0.48
LMBWR	5.51 ± 1.40	1.94 ± 2.89	-0.51 ± 0.24
	Second fertilization period (May 23 – June 1)		
TrIR	2.52 ± 0.54	5.99 ± 11.95	-0.48 ± 0.27
TrBWR	2.90 ± 0.61	2.58 ± 1.76	-0.63 ± 0.27
LMIR	4.12 ±0.79	1.47 ±1.04	-0.46 ±0.55
LMBWR	10.70 ± 1.11	1.79 ± 1.30	-0.54 ± 0.20

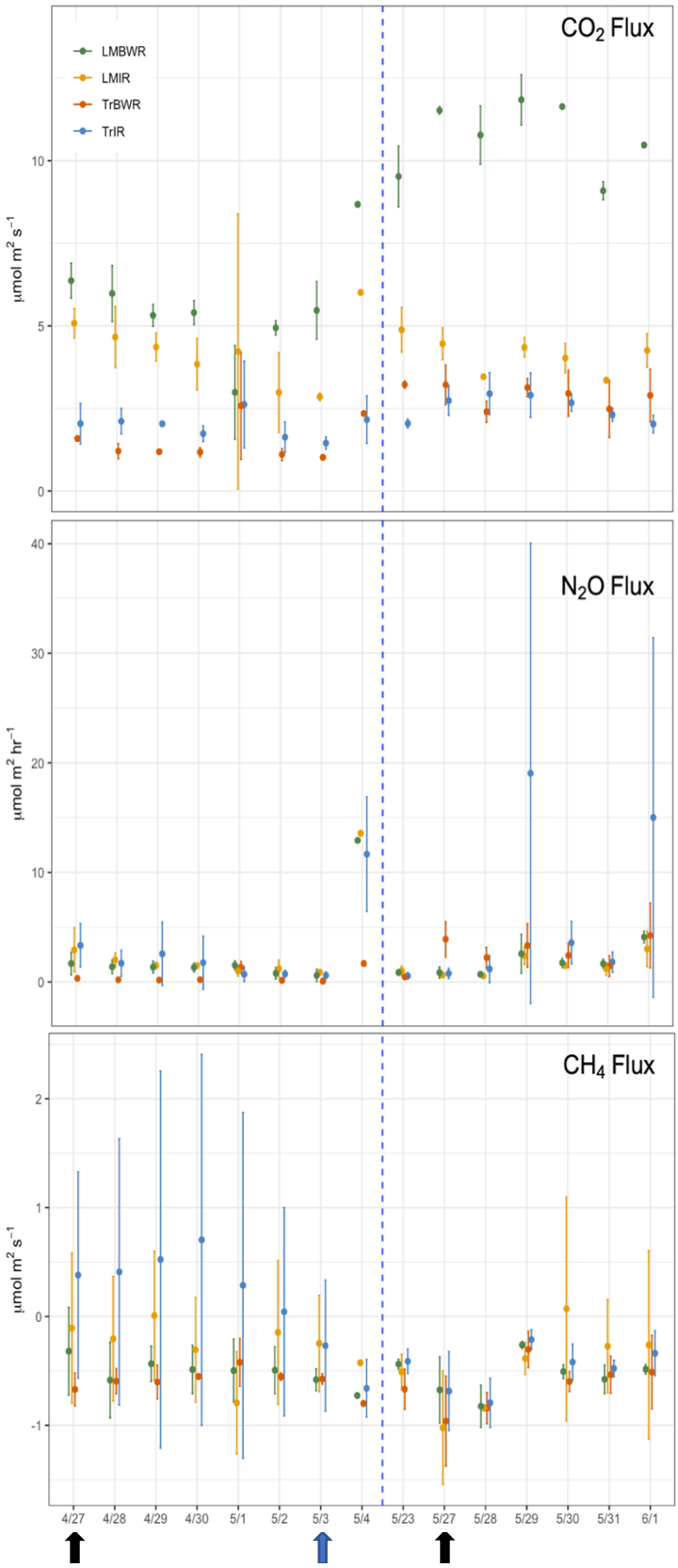

Figure 4. Temporal changes of daily average GHG flux (CO_2, N_2O, and CH_4) measurements in 2019 during early growing season taken in traditional in row (TrIR), traditional between the row (TrBWR), living mulch in row (LMIR) and living mulch between the row (LMBWR). Black arrows represent twice fertilizer application (4/27 and 5/27), and blue arrow represents one irrigation event (5/3) during measuring time.

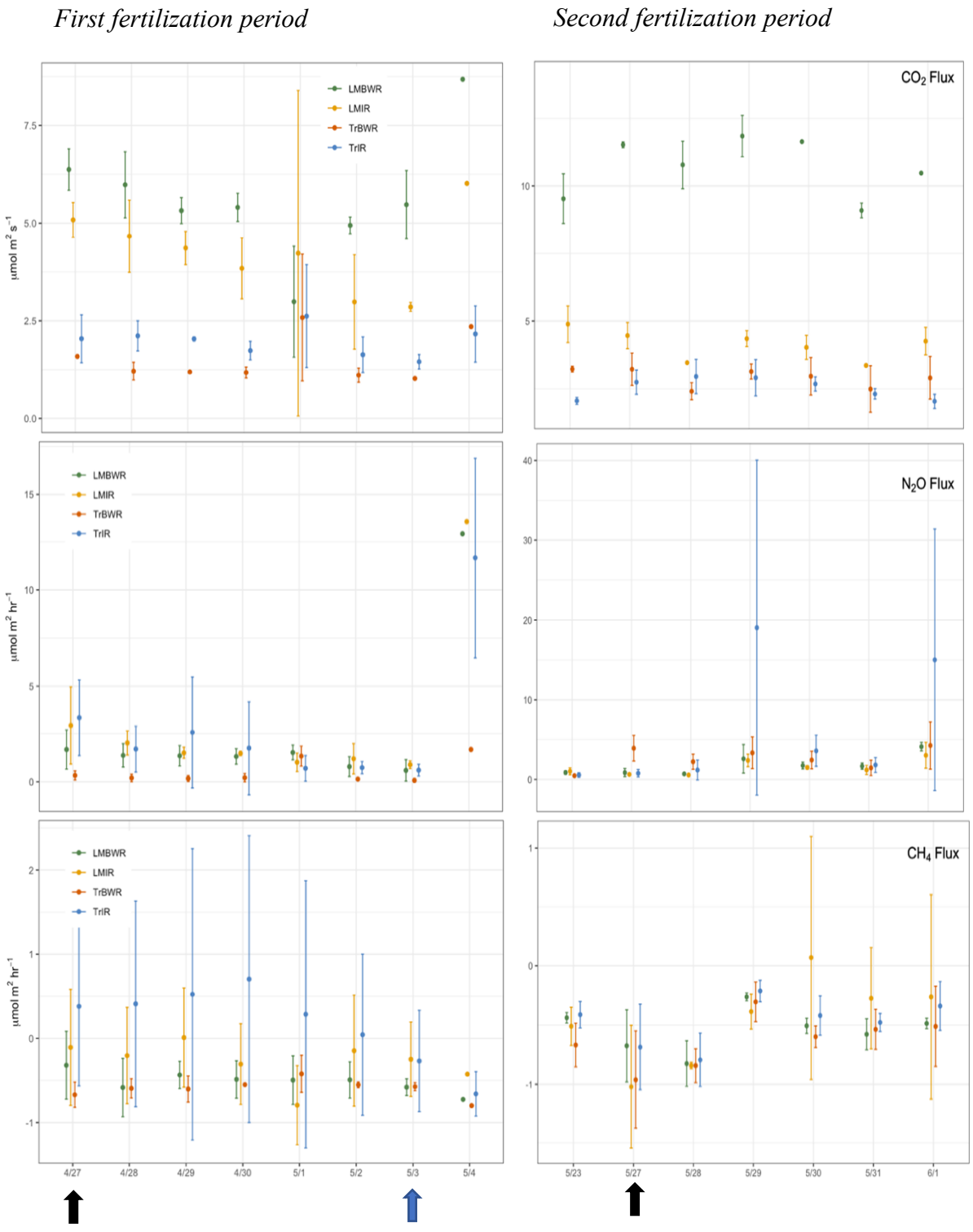

Figure 4. Temporal changes of daily average GHG flux (CO_2, N_2O, and CH_4) measurements in 2019 in both first and second fertilization period in early growing season taken in traditional in row (TrIR), traditional between the row (TrBWR), living mulch in row (LMIR), and living mulch between the row (LMBWR). Black arrows represent twice fertilizer application (4/27 and 5/27), and blue arrow represents one irrigation event (5/3) during measuring time.

We observed the highest N_2O emissions from TrIR (3.93 μmol m^2 hr^{-1}, Table 9) in 2019. Peters et al. (2020) observed higher N_2O flux in LM compared to Tr in 2016 and 2017. Unlike the previous study, we did not observe the highest N_2O emissions from LMBWR in 2019. Comparing N_2O emissions between in-row and between-row, higher N_2O emissions were found in TrIR than in TrBWR ($p < 0.01$, Table 12). In LM, in-row and between-row measurements did not show significant N_2O difference in 2019 (LMIR-LMBWR: $p = 0.90$, Table 12). Around the first fertilization period, the highest N_2O flux was observed in LMIR (2.33 μmol m^2 hr^{-1}), which was significantly higher than those in TrBWR ($p < 0.05$, Table 12). In the second fertilization period, we observed significantly higher N_2O fluxes in TrIR (5.99 μmol m^2 hr^{-1}) compared to TrBWR, LMIR, and LMBWR (Table 13). Higher N_2O emissions were observed in TrIR than TrBWR in both first and second fertilization periods (first: TrIR-TrBWR: $p < 0.001$; second: TrIR-TrBWR: $p < 0.05$, Table 13). However, LMIR and LMBWR did not show significant N_2O emissions generated in both first and second fertilization periods (first: LMIR-LMBWR: $p = 0.70$; second: LMIR-LMBWR: $p = 0.48$, Table 13).

Table 11. Mean N_2O flux Welch t test (n =217) between select two measurements in 2019.

Groups	*Difference (μmol m^{-2} hr^{-1})*	*95% Lower CI*	*95% Upper CI*	*t*	*df*	*p-value*
			2019			
TrIR-TrBWR	2.54	0.92	4.16	3.09	148.79	2.4×10^{-3} **
TrIR-LMIR	1.98	0.26	3.71	2.27	151.64	2.5×10^{-2} *
TrIR-LMBWR	2.06	0.34	3.78	2.37	152.36	1.9×10^{-2} *
TrBWR-LMIR	-0.56	-1.59	0.48	-1.08	53.62	0.28
TrBWR-LMBWR	-0.48	-1.49	0.53	-0.95	54.58	0.35
LMIR-LMBWR	0.075	-1.10	1.25	0.13	59.93	0.90

*p < 0.05, **p < 0.01, ***p < 0.001

Table 12. Mean N_2O flux Welch t test between certain two measurements among TrIR, TrBWR, LMIR, and LMBWR in in first (n = 119) and second (n = 98) fertilization periods in 2019.

Groups	Difference (μmol m^{-2} hr^{-1})	95% Lower CI	95% Upper CI	t	df	p-value
			2019 First fertilization period (April 27 – May 4)			
TrIR-TrBWR	1.90	1.02	2.62	4.50	78.98	2.3×10^{-5} ***
TrIR-LMIR	-0.11	-1.81	1.60	-0.13	25.41	0.90
TrIR-LMBWR	0.29	-1.35	1.93	0.37	26.40	0.72
TrBWR-LMIR	-1.92	-3.50	-0.35	-2.58	17.00	1.9×10^{-2} *
TrBWR-LMBWR	-1.53	-3.03	-0.02	-2.14	17.10	4.7×10^{-2} *
LMIR-LMBWR	0.40	-1.67	2.47	0.39	31.93	0.70
			2019 Second fertilization period (May 23 – June 1)			
TrIR-TrBWR	3.41	0.09	6.74	2.05	62.98	4.4×10^{-2} *
TrIR-LMIR	4.52	1.28	7.76	2.79	58.15	7.1×10^{-3} **
TrIR-LMBWR	4.20	0.93	7.47	2.53	59.78	1.3×10^{-2} *
TrBWR-LMIR	1.11	-0.03	2.24	2.03	21.05	5.6×10^{-2}
TrBWR-LMBWR	0.79	-0.42	2.00	1.35	23.93	0.19
LMIR-LMBWR	-0.32	-0.71	0.60	-0.71	24.77	0.48

*p < 0.05, **p < 0.01, ***p < 0.001

We observed a statistically significantly smaller CH_4 sink in TrIR (-0.08 μmol m^2 hr^{-1}, Table 9) compared to TrBWR, LMIR, and LMBWR in 2019 (TrIR-TrBWR: $p < 0.001$; TrIR-LMIR: $p < 0.05$; TrIR-LMBWR: $p < 0.001$, Table 14). Regarding CH_4 flux between in-row and between-row, we observed a larger CH_4 sink in TrIR compared with TrBWR ($p < 0.001$, Table 14). However, in LM, we did not observe a significant difference in soil CH_4 flux between LMIR and LMBWR (p =0.09, Table 14). In both first and second fertilization periods, we observed the highest CH_4 uptake from TrBWR (first: -0.58 μmol m^2 hr^{-1}, second: -0.63 μmol m^2 hr^{-1}, Table 15). Comparing CH_4 flux generated between in-row and between-row, significant larger CH_4 sink was observed in TrBWR compared with TrIR in the first fertilization period ($p < 0.001$, Table 15). However, LMIR and LMBWR did not show CH_4 flux difference in both first and second fertilization periods (early: LMIR-LMBWR: $p = 0.07$; late: LMIR-LMBWR: $p = 0.63$, Table 15).

Table 13. Mean CH_4 flux Welch t test (n = 217) between select two measurements in 2019.

Groups	*Difference (μmol m^{-2} hr^{-1})*	*95% Lower CI*	*95% Upper CI*	*t*	*df*	*p-value*
			2019			
TrIR-TrBWR	0.54	0.34	0.72	5.40	150.06	2.5×10^{-7} ***
TrIR-LMIR	0.27	0.017	0.53	2.12	94.09	3.6×10^{-2} *
TrIR-LMBWR	0.45	0.25	0.64	4.52	151.69	1.2×10^{-5} ***
TrBWR-LMIR	-0.40	-0.46	-0.05	-2.56	39.19	1.5×10^{-2} *
TrBWR-LMBWR	-0.08	-0.19	0.026	-1.51	59.68	0.13
LMIR-LMBWR	0.17	-0.03	0.38	1.71	40.55	9.4×10^{-2}

*p < 0.05, **p < 0.01, ***p < 0.001

Table 14. Mean CH_4 flux Welch t test between certain two measurements among TrIR, TrBWR, LMIR, and LMBWR in in first (n = 119) and second (n = 98) fertilization periods in 2019.

Groups	Difference (μmol m^{-2} hr^{-1})	95% Lower CI	95% Upper CI	t	df	p-value
			2019 First fertilization period (April 27 – May 4)			
TrIR-TrBWR	0.84	0.53	1.15	5.40	72.06	8.2×10^{-7} ***
TrIR-LMIR	0.51	0.13	0.90	2.68	68.87	9.2×10^{-3} **
TrIR-LMBWR	0.77	0.44	1.09	4.71	80.66	1.0×10^{-5} ***
TrBWR-LMIR	-0.32	-0.58	-0.07	-2.67	13.19	1.5×10^{-2} *
TrBWR-LMBWR	-0.072	-0.21	0.06	-1.11	24.40	0.28
LMIR-LMBWR	0.25	-0.02	0.52	1.92	23.34	0.67
			2019 Second fertilization period (May 23 – June 1)			
TrIR-TrBWR	0.15	-0.02	0.32	1.90	19.53	7.3×10^{-2}
TrIR-LMIR	-0.016	-0.34	0.31	-0.11	14.54	0.92
TrIR-LMBWR	0.061	-0.07	0.20	0.94	25.24	0.35
TrBWR-LMIR	-0.17	-0.52	0.17	-1.04	19.06	0.31
TrBWR-LMBWR	-0.093	-0.28	0.10	-1.02	24.01	0.32
LMIR-LMBWR	0.078	-0.25	0.41	0.49	16.49	0.63

*p < 0.05, **p < 0.01, ***p < 0.001

GHG fluxes in TrIR plots in 2019

As explained earlier, during the first fertilization period, three chambers in TrIR1 (TrIR1-1, TrIR1-2, and TrIR1-3) received N fertilizer at the rate of 50 kg ha^{-1}. During the second fertilization period, eight chambers in both TrIR1 and TrIR2 received fertilizer application, ranging from 0-200 kg ha^{-1} (TrIR1-0: 0 kg ha^{-1}; TrIR1-1: 100 kg ha^{-1}; TrIR1-2: 150 kg ha^{-1}; TrIR1-3: 200 kg ha^{-1}, TrIR2-0: 0 kg ha^{-1}; TrIR2-1: 100 kg ha^{-1}; TrIR2-2: 150 kg ha^{-1}; TrIR2-3: 200 kg ha^{-1}). None of the eight chambers showed statistically significantly different CO_2 emissions in the first fertilization period (Figure 6). For N_2O, three chambers in TrIR1 (TrIR1-1, TrIR1-2, and TrIR1-3) which received N fertilizer (urea) twice in both periods all showed higher emissions than chambers in TrIR2 in both periods. In either TrIR1 or TrIR2, two chambers that received the highest and second highest amount of N fertilizer did not differ significantly for N_2O. Three chambers which received fertilization twice (TrIR1-1, TrIR1-2, and TrIR1-3) showed significantly higher N_2O than their paired chambers (TrIR2-1, TrIR2-2, and TrIR2-3) which only received fertilization once. For CH_4, TrIR2-0 that did not receive any N fertilizer showed significantly higher CH_4 emissions (2.78 μmol m^2 hr^{-1}) compared to those in the other three chambers in TrIR2 (Table 16).

During the second fertilization period, three chambers under TrIR1 that had already received fertilizer earlier did not differ significantly for CO_2 emissions during the second fertilization period. However, significantly higher CO_2 emissions were observed in TrIR2-3 compared to TrIR2-1 and TrIR2-0 in the second fertilization period (Table 16). The highest average N_2O emissions were observed in TrIR1-3 (16.18 μmol m^2 hr^{-1}), which received the highest N fertilizer amount (250 kg ha^{-1}) among all eight plots in TrIR during the second fertilization period. Comparing N_2O emissions between TrIR1 and TrIR2, higher N_2O flux was observed in TrIR1 than in TrIR2 in both periods (Table 16). This could originate from the difference in N fertilizer inputs. Furthermore, soils in TrIR1 served as a larger CH_4 sink than those in TrIR2 which received fertilizer application only once.

Table 15. Average and standard deviation of trace gas fluxes (CO_2: µmol m^2 s^{-1}; N_2O and CH_4: µmol m^2 hr^{-1}) for eight chambers in TrIR during the first and second fertilization periods during first (n = 204) and second (n = 168) fertilization periods growing season in 2019.

	CO_2	N_2O	CH_4
Early growing season (April 22 - July 5)			
TrIR1-0	1.93 ± 0.45	1.77 ± 2.21	-0.34 ± 0.40
TrIR1-1	2.04 ± 0.59	4.24 ± 4.19	-0.62 ± 0.17
TrIR1-2	1.85 ± 0.54	4.51 ± 6.05	-0.56 ± 0.15
TrIR1-3	1.74 ± 0.36	3.80 ± 3.35	-0.53 ± 0.12
TrIR2-0	1.73 ± 0.44	0.54 ± 0.29	2.78 ± 1.34
TrIR2-1	1.83 ± 0.47	0.61 ± 0.21	0.27 ± 0.42
TrIR2-2	1.68 ± 0.55	1.19 ± 0.49	-0.43 ± 0.21
TrIR2-3	2.24 ± 0.40	1.05 ± 0.95	0.84 ± 0.69
Late growing season (July 12 – August 16)			
TrIR1-0	2.45 ± 0.28	2.13 ± 1.38	-0.64 ± 0.22
TrIR1-1	2.46 ± 0.53	10.29 ± 13.04	-0.55 ± 0.16
TrIR1-2	2.19 ± 0.30	10.90 ± 15.31	-0.62 ± 0.25
TrIR1-3	2.68 ± 0.5	16.18 ± 24.38	-0.63 ± 0.28
TrIR2-0	2.19 ± 0.30	0.97 ± 1.30	-0.44 ± 0.38
TrIR2-1	2.26 ± 0.32	1.99 ± 1.81	-0.34 ± 0.16
TrIR2-2	2.63 ± 0.52	2.65 ± 3.31	-0.35 ± 0.18
TrIR2-3	2.99 ± 0.74	3.12 ± 2.96	-0.41 ± 0.21

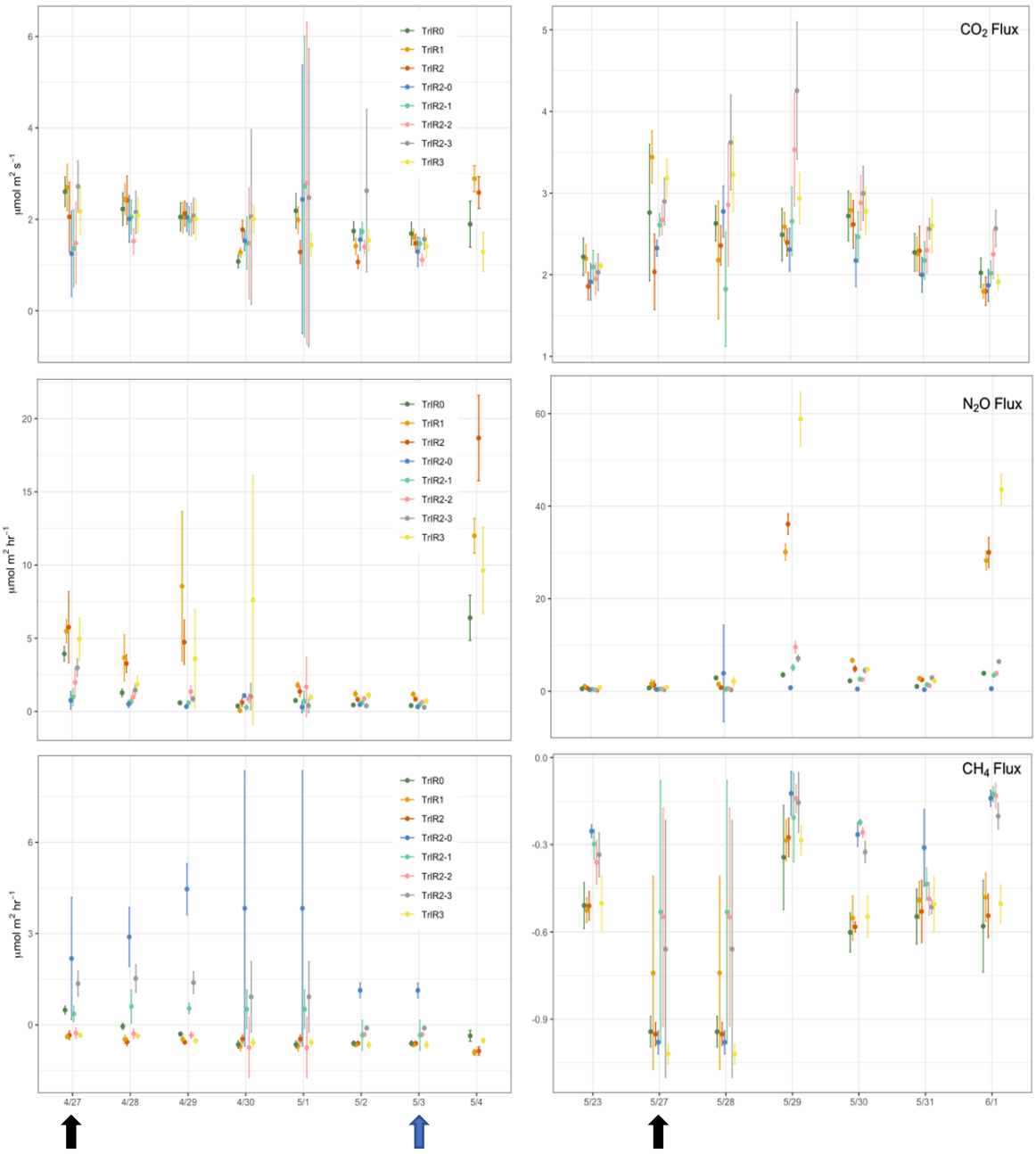

Figure 5. Temporal changes of daily average GHG (CO_2, N_2O, and CH_4) flux measurements during the first and second fertilization periods in 2019 growing season for eights treatments in TrIR. Black arrows represent twice fertilizer application (4/27 and 5/27), and blue arrow represents one irrigation event (5/3) during measuring time.

Discussion

CO_2 and N_2O flux

We observed significantly higher CO_2 emissions in both LMIR and LMBWR compared with TrIR and TrBWR, respectively. Our finding differs from the past study where higher CO_2 fluxes were only found in LMBWR compared with TrBWR (Peters et al., 2020). There might be two potential reasons explaining why we also observed higher CO_2 emissions in LMIR compared to TrIR and TrBWR, respectively. The first reason is that we conducted our experiment in an intensive daily manner with *in-situ* measurement, which made it possible for us to observe the difference better in 2019. The second potential reason is the change in soil C and N in the rows of maize as well as in between the rows after the three-year incorporation of LM in the soil. In 2019, soils in LMIR had a larger C but a lower N during the early growing season when we conducted our measurements (Figure 7). Although between the row is where white clover is present, it is clear that soils in in the rows of maize were also significantly different from those in the Tr system in 2019.

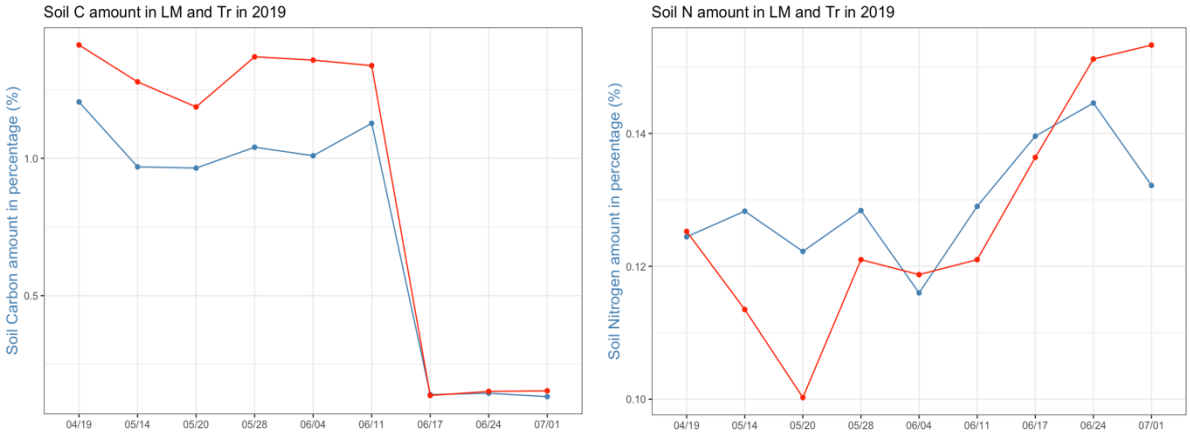

Figure 6. Soil C and N amount measured in rows of maize under LM and Tr in 2019. Red line represents LM and blue line represents Tr.

We observed higher N_2O emissions in LM in 2018 compared to the other three treatments (CC, CR, and Tr), as found in Peters et al. (2020) in 2016 and 2017. The largest N_2O fluxes were observed in LM on June 20th, which was likely due to the elevated soil N added as the white clover decomposed. From observing the relationship between the soil N amount and white clover biomass in the soil, the soil N content increased as white clover biomass decreased between the end of May to mid-July in 2018 (Figure 8). In 2018, only one soil N measurement was taken between mid-June to mid-July, and it appears that maximum soil content was on July 10th (Figure 8). However, more frequent soil N observations in 2019 illustrate the changes of soil N amount better. From June 11th to Jun 24th, the rate of soil N amount increase is one of the highest when we observed the maximum N_2O flux generated in LM (Figure 7). Therefore, N_2O production in LM might also be associated with the rate of soil N content increase rather than only with the actual soil N content.

However, we did not observe the highest N_2O emissions in between rows of maize under LM in 2019. As discussed, greater soil N was observed in Tr than LM from April to the end of

May, when we conducted measurements (Figure 7). Soil N in LM increased from the end of May to mid-July due to the decomposition of white clover, which corresponds perfectly to the higher N_2O flux observed in late June to early July in LM in 2018 (Figure 2). This is similar to what Peters et al. (2020) observed in 2016 and 2017. However, in 2019, since we focused our measurements in the early growing season during fertilization periods, added N provided by clover in LM still did not outweigh the N inputs in Tr and subsequently we did not observe higher N_2O emissions in LM compared to Tr in 2019.

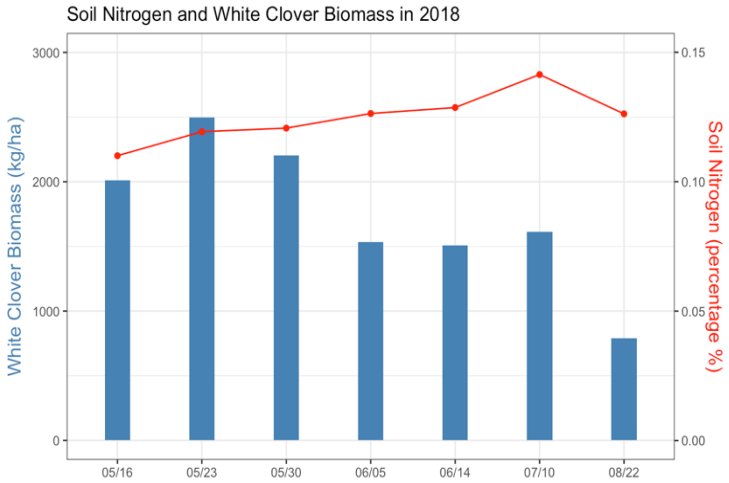

Figure 7. The relationship between soil nitrogen content (percentage %) and white clover biomass(kg/ha) in 2018.

Among eight chambers of TrIR in 2019, the chamber that received the greatest amount of fertilizer emitted the highest CO_2 flux. For N_2O, the chamber with the greatest amount of N inputs emitted the highest N_2O emissions. Among the three cover crop systems, higher N_2O flux emitted in LM compared to CC and CR in 2018 could be related to greater mineralizable C in the soil. Mineralizable C is used as a substrate to stimulate N_2O emissions generated from the denitrification process (Mitchell et al., 2013). Comparing CO_2 and N_2O emissions between leguminous (CC) and non-leguminous cover crops (CR), no significant difference was observed between those two from observations in 2018. However, studies suggest that cover crops with N fixing ability tend to increase the amount of soil inorganic C, whereas cover crops with no N fixing ability leads to N immobilization (Schmatz et al. 2020).

CH_4 flux

Soils in cover crop systems were observed as higher CH_4 sinks compared to Tr in 2018. Among the three cover crop systems, slightly lower CH_4 consumption in CR potentially resulted from its higher C/N ratio due to its inability to fix N. CR most likely had a higher soil carbon amount, which may have stimulated CH_4 emissions under anaerobic conditions (Le Mer and Roger, 2001). Previous studies also found that soils with increased NH_4^+ addition leads to decreased CH_4 uptake (Boeckx & Van Cleemp. 1996). The similarity in physical properties of NH_4^+ and CH_4 molecules allow them to compete for binding sites in the Methane Mono-Oxygenase (MMO) enzyme. NH_4^+ inhibition effects refer to the fact that NH_4^+, as a more aggressive competing substrate, can inhibit CH_4 oxidation process (Gulledge et al. 1997). Future studies should include the measurements of soil NH_4^+ and C/N ratio of the soil to further

investigate their impacts on CH_4 uptake ability.

Intensive land management activities could also influence the CH_4 uptake ability. In 2018, decreasing CH_4 uptake occurred from April 22nd to early May, suggesting that soil disturbance event, such as planting maize and increased N inputs from fertilizer during this time affected the role of soil as absorbing CH_4 (Bronson & Mosier, 1994; Conrad & Rothfuss, 1991; Dunfield & Knowles, 1995). In 2019, a higher CH_4 sink from between-row than in-row was observed under both LM and Tr systems. This indicates that higher soil N in the in-row may have inhibited CH_4 uptake and resulted in a smaller CH_4 sink. However, instead of being the largest CH_4 sink, TRIR2-0, the chamber which did not receive any N inputs, served as the smallest CH_4 sink among the eight chambers in TrIR. Furthermore, chambers that received higher levels of N fertilizers tended to be larger CH_4 sinks than those that received lower N. Additional experiments are needed to better understand what fertilization pattern to enhance soil CH_4 sink potential so that mitigation potential can be enhanced in agriculture.

In order to better assess the mitigation potential of different cover crop systems compared to conventional agricultural system, we also compared four agricultural practices with a net CO_2e. In our study, short-term mitigation effects from larger CH_4 sink, increased soil carbon sequestration, reduced fertilizer and herbicides application are still not capable of counteracting higher CO_2 and N_2O emissions generated in the field. The net CO_2e from CC, CR, LM, and Tr are 17,323, 17,129, 30,101, and 11,042 kg ha^{-1} yr^{-1}, respectively.

Table 16. Cumulative Net CO_2e in four agricultural practices in 2018

Treatment	*CC*	*CR*	*LM*	*Tr*
kg ha^{-1} yr^{-1}	17,323	17,129	30,101	11,402

One limitation in our study is the lack of soil microbial data. Including soil microbial measurements might add insights in understanding GHG fluxes variations occurred between cover crop systems and conventional agricultural system. In order to better understand the live clover impacts on GHG emissions, both long-term soil GHG observation and microbial level laboratory studies are needed. From the results of this study, we observed increased soil CO_2 emissions also from LMIR, which comes from the accelerated decomposition of native soil due to clover incorporation. Studies have shown that incorporating fresh organic matter such as clover residue could stimulate mineralization of soil organic matter, which is named as priming effect (Fontaine et al. 2003; Bingeman et al. 1953). Future studies should also investigate the microbial mechanism of priming effects induced by cover crop residues. Moreover, soil parameters were only collected as total C and total N amounts in our study. Future studies should also include the measurements of both particulate and mineral soil organic matter types under different cover crop systems. Different types of soil organic matter measurements could better evaluate the type of organic matter added to the soil by cover crops, their susceptibility to further decomposition and CO_2 and N_2O emissions. A more comprehensive N budget should also be included in future studies to better evaluate the mitigation potential comparison between legume and non-legume cover crops. Reducing GHG emissions from agriculture is complex since the success of realizing mitigation potential through cover crop establishment is site-specific. Spatial heterogeneity acts as barriers to wider adoption of cover crops regarding different local conditions. There is no one-size-fits all

solution, and future studies still need to fully evaluate both locally and globally about barriers and opportunities for successful cover crop implementation.

Conclusion

From this study, we observed a larger CH_4 sink in soil with cover crops than in a conventional agricultural system. Cover crops provide benefits in improving soil and water quality, such as increased soil C, reduced soil erosion and nitrate leaching. From the findings of this study, the implementation of cover crops can add another benefit as being the CH_4 sink. However, in our study site, mitigation effects from CH_4 sink are still not capable of counteracting higher CO_2 and N_2O emissions generated in the cover crop systems than conventional agricultural system. In order to assess climate change mitigation potential from agriculture, it is important to analyze the three GHG fluxes holistically and understand the impacts of different practices in more detail.

References

Andrews, J. S., Sanders, Z. P., Cabrera, M. L., Saha, U. K., & Hill, N. S. (2018). Nitrogen dynamics in living mulch and annual cover crop corn production systems. *Agronomy Journal*, *110*(4), 1309–1317. https://doi.org/10.2134/agronj2017.10.0609

Aydinalp, C., & Cresser, M. S. (2008). Agriculture Land use change (including biomass burning) The Effects of Global Climate Change on Agriculture. *Agric. & Environ. Sci*, *3*(5), 672–676.

Basche, A. D., Miguez, F. E., Kaspar, T. C., & Castellano, M. J. (2014). Do cover crops increase or decrease nitrous oxide emissions? a meta-analysis. *Journal of Soil and Water Conservation*, *69*(6), 471–482. https://doi.org/10.2489/jswc.69.6.471

Bing C.W., Varner J.E., Martin W.P. (1953). The effect of the addition of organic materials on the decomposition of an organic soil. *Soil Sci Soc Am J*. (17), 34-38.

Bronson K.F., Mosier A.R., (1994). Suppression of methane oxidation in aerobic soil by nitrogen fertilizers; nitrification inhibitors; and urease inhibitors, *Biol. Fert. Soils.* (17), 263–268.

Boeckx Pascal & Van Cleemput Oswald. (1996). Methane oxidation in neutral landfill cover soil: influence of soil moisture content, temperature and nitrogen turn-over, *J.Environ. Qual.* (25), 178-183.

Conrad R., Rothfuss F. (1991). Methane oxidation in the soil surface layer of a flooded ricefield and the effect of ammonium, *Biol. Fert. Soils*. 12, 28–32.

Dunfield P., Knowles R. (1995). Kinetics of inhibition of methane oxidation by nitrate, nitrite, and ammonium in a humisol, *Appl. Environ. Microbiol*. (61), 3129–3135.

Gulledge, J., Doyle, A. P., & Schimel, J. P. (1997). Different NH_4^+ inhibition patterns of soil CH_4 consumption: A result of distinct CH_4-oxidizer populations across sites. *Soil Biology and Biochemistry*, *29*(1), 13–21. https://doi.org/10.1016/S0038-0717(96)00265-9

IPCC. (2007). Summary for Policymakers. In: Climate Change 2007: C*ontribution of Working Group I to the Fourth Assessment Report of the Intergovernmental Panel on Climate Change* [Solomon, S., D. Qin, M. Manning, Z. Chen, M. Marquis, K.B. Averyt, M. Tignor and H.L. Miller (eds.)]. Cambridge University Press, Cambridge, United Kingdom and New York, NY, USA.

IPCC. (2013). *Climate Change 2013: The Physical Science Basis. Contribution of Working Group I to the Fifth Assessment Report of the Intergovernmental Panel on Climate Change* [Stocker, T.F., D. Qin, G.-K. Plattner, M. Tignor, S.K. Allen, J. Boschung, A. Nauels, Y. Xia, V. Bex and P.M. Midgley (eds.)]. Cambridge University Press, Cambridge,

United Kingdom and New York, NY, USA, 1535 pp.

IPCC. (2014). Climate Change 2014: Synthesis Report. Contribution of Working Groups I, II and III to the Fifth Assessment Report of the Intergovernmental Panel on Climate Change [Core Writing Team, R.K. Pachauri and L.A. Meyer (eds.)]. IPCC, Geneva, Switzerland, 151 pp.

Jarecki, M. K., Parkin, T. B., Chan, A. S. K., Kaspar, T. C., Moorman, T. B., Singer, J. W., … Jones, R. (2009). Cover crop effects on nitrous oxide emission from a manure-treated Mollisol. *Agriculture, Ecosystems and Environment*, *134*(1–2), 29–35. https://doi.org/10.1016/j.agee.2009.05.008

Johnson, R. (2018). Greenhouse Gas Emissions and Sinks in U . S . Agriculture. 1–2.

Kim, S. Y., Gutierrez, J., & Kim, P. J. (2012). Considering winter cover crop selection as green manure to control methane emission during rice cultivation in paddy soil. *Agriculture, Ecosystems and Environment*, *161*, 130–136. https://doi.org/10.1016/j.agee.2012.07.026

Lal R. (2004). Carbon emissions from farm operations. *Environment International*. 30, 981-990.

Le Mer, J., & Roger, P. (2001). Production, oxidation, emission and consumption of methane by soils: A review. *European Journal of Soil Biology*, *37*(1), 25–50. https://doi.org/10.1016/S1164-5563(01)01067-6

Le Quéré, C., Andrew, R. M., Friedlingstein, P., Sitch, S., Pongratz, J., Manning, A. C., Korsbakken, J. I., Peters, G. P., Canadell, J. G., Jackson, R. B., Boden, T. A., Tans, P. P., Andrews, O. D., Arora, V. K., Bakker, D. C. E., Barbero, L., Becker, M., Betts, R. A., Bopp, L., Chevallier, F., Chini, L. P., Ciais, P., Cosca, C. E., Cross, J., Currie, K., Gasser, T., Harris, I., Hauck, J., Haverd, V., Houghton, R. A., Hunt, C. W., Hurtt, G., Ilyina, T., Jain, A. K., Kato, E., Kautz, M., Keeling, R. F., Klein Goldewijk, K., Körtzinger, A., Landschützer, P., Lefèvre, N., Lenton, A., Lienert, S., Lima, I., Lombardozzi, D., Metzl, N., Millero, F., Monteiro, P. M. S., Munro, D. R., Nabel, J. E. M. S., Nakaoka, S., Nojiri, Y., Padin, X. A., Peregon, A., Pfeil, B., Pierrot, D., Poulter, B., Rehder, G., Reimer, J., Rödenbeck, C., Schwinger, J., Séférian, R., Skjelvan, I., Stocker, B. D., Tian, H., Tilbrook, B., Tubiello, F. N., van der Laan-Luijkx, I. T., van der Werf, G. R., van Heuven, S., Viovy, N., Vuichard, N., Walker, A. P., Watson, A. J., Wiltshire, A. J., Zaehle, S., and Zhu, D.: Global Carbon Budget 2017, *Earth Syst. Sci. Data*, 10, 405–448, https://doi.org/10.5194/essd-10-405-2018, 2018.

Lu Y., Wassmann R., Neue H.U., Huang C. (1999). Impact of phosphorus supply on root exudation, aerenchyma formation and methane emission of rice plants, *Bio-geochemistry* 47, 203–218.

Melancon Merritt. (2014). Dedication of J. Phil Campbell Research and Education Center in Watkinsville. *Georgia Seed Development*. http://gsdc.com/news/dedication-j-phil-campbell-research-and-education-center-in-watkinsville

Mitchell D.C., Castellano M.J., Sawyer J.E., Pantoja J. (2013). Cover crop effects on nitrous oxide emissions: role of minerlizable carbon. *Soil Science Society of America Journal.* 10.2136/sssaj2013.02.0074

Paustian, K., Lehmann, J., Ogle, S., Reay, D., Robertson, G. P., & Smith, P. (2016). Climate-smart soils. *Nature*, 532(7597), 49–57. https://doi.org/10.1038/nature17174

Peters, S. J., Saikawa, E., Markewitz, D., Sutter, L., Avramov, A., Sanders, Z. P., … Hill, N. S. (2020). Soil trace gas fluxes in living mulch and conventional agricultural systems. *Journal of Environmental Quality*, 1–13. https://doi.org/10.1002/jeq2.20041

Ravishankara, A. R., Daniel, J. S., & Portmann, R. W. (2009). Nitrous oxide (N_2O): The dominant ozone-depleting substance emitted in the 21st century. *Science*, *326*(5949), 123–125. https://doi.org/10.1126/science.1176985

Saunois, M., Stavert, A. R., Poulter, B., Bousquet, P., Canadell, J. G., Jackson, R. B., … Houweling, S. (2020). *The Global Methane Budget 2000 – 2017*. 1561–1623.

Schomberg, H.H., D.M. Endale, A. Calegari, R. Peixoto, M. Miyazawa, and M.L. Cabrera. (2006). Influence of cover crops on potential nitrogen availability to succeeding crops in a Southern Piedmont soil. *Biol. Fertil. Soils 42*: 299–307. doi:10.1007/s00374-005-0027-8

Shcherbak, I., Millar, N., & Robertson, G. P. (2014). Global metaanalysis of the nonlinear response of soil nitrous oxide (N_2O) emissions to fertilizer nitrogen. *Proceedings of the National Academy of Sciences of the United States of America*, *111*(25), 9199–9204. https://doi.org/10.1073/pnas.1322434111

Smith P., M. Bustamante, H. Ahammad, H. Clark, H. Dong, E.A. Elsiddig, H. Haberl, R. Harper, J. House, M. Jafari, O. Masera, C. Mbow, N.H. Ravindranath, C.W. Rice, C. Robledo Abad, A. Romanovskaya, F. Sperling, and F. Tubiello, 2014: Agriculture, Forestry and Other Land Use (AFOLU). In: Climate Change 2014: Mitigation of Climate Change. Contribution of Working Group III to the Fifth Assessment Report of the Intergovernmental Panel on Climate Change [Edenhofer, O., R. Pichs-Madruga, Y. Sokona, E. Farahani, S. Kadner, K. Seyboth, A. Adler, I. Baum, S. Brunner, P. Eickemeier, B. Kriemann, J. Savolainen, S. Schlömer, C. von Stechow, T. Zwickel and J.C. Minx (eds.)]. Cambridge University Press, Cambridge, United Kingdom and New York, NY, USA.

Snyder, C. S., Bruulsema, T. W., Jensen, T. L., and Fixen, P. E. (2009). Review of greenhouse gas emissions from crop production systems and fertilizer management effects, *Agr. Ecosyst. Environ*, 133, 247–266.

Smith M.S., Tiedje J.M. (1979). Phases of denitrification following oxygen depletion in soil. *Soil Biology and Biochemistry*, 11(3), 261-267.

Tian, H., Xu, R., Canadell, J. G., Thompson, R. L., Winiwarter, W., Suntharalingam, P., … Yao, Y. (2020). A comprehensive quantification of global nitrous oxide sources and sinks. *Nature*, *586*(7828), 248–256. https://doi.org/10.1038/s41586-020-2780-0

Tribouillois H., Constantin J., Justes E. (2017). Cover crops mitigate direct greenhouse gases balance but reduce drainage under climate change scenarios in temperate climate with dry summers. *Global Change Biology*. 24, 2513-2529.

Tubiello, F. N., Salvatore, M., Ferrara, A., Rossi, S., Biancalani, R., Condor Golec, R. D., ... Srivastava, N. (2015). The Contribution of Agriculture, Forestry and other Land Use activities to Global Warming, 1990-2010: Not as high as in the past. *Global Change Biology*, 2655–2660.

Turner, P. A., Baker, J. M., Griffis, T. J., & Venterea, R. T. (2016). Impact of Kura Clover Living Mulch on Nitrous Oxide Emissions in a Corn–Soybean System. *Journal of Environment Quality*, *45*(5), 1782. https://doi.org/10.2134/jeq2016.01.0036

Zemenchik, R.A., Albrecht, K.A., Boerboom, C.M., and Lauer, J.G. (2000). Corn production with kura clover as a living mulch. *Agron. J.* 92:698–705. doi:10.2134/agronj2000.924698x